

THE SLD CALORIMETER SYSTEM *

A. C. BENVENUTI

INFN, Sezione di Bologna, I-40126 Bologna, Italy

L. PIEMONTESE

INFN, Sezione di Ferrara and Università di Ferrara, I-441 00 Ferrara, Italy

A. CALCATERRA, R. DE SANGRO, P. DE SIMONE, I. PERUZZI and M. PICCOLO
Lab. Nazionali di Frascati *dell'INFN*, I-00044 Frascati (Roma), Italy

P. N.-BURROWS, W. BUSZA, S. L. CARTWRIGHT, J. I. FRIEDMAN, S. FUESS,
S. GONZALEZ, T. HANSL-KOZANECKA, H. W. KENDALL, A. LATH, T. LYONS,
L. S. OSBORNE, L. ROSENSON, U. SCHNEEKLOTH, F. E. TAYLOR,
R. VERDIER, D. WILLIAMS and J. M. YAMARTINO
Massachusetts Institute of Technology, Cambridge, MA 02139, USA

N. BACCHETTA, D. BISELLO, A. CASTRO, M. LORETI, L. PESCARA and J. WYSS
INFN, Sezione di Padova and Università di Padova, I-35100 Padova, Italy

B. ALPAT, R. BATTISTON, G. M. BILEI, R. DELL'ORSO, G. MANTOVANI,
M. PAULUZZI and L. SERVOLI
INFN, Sezione di Perugia and Università di Perugia, I-061 00 Perugia, Italy

M. CARPINELLI, R. CASTALDI, C. VANNINI and P. G. VERDINI
INFN, Sezione di Pisa and Università di Pisa, I-56010 San Piero a Grado, Italy

B. L. BYERS, D. KHARAKH, R. L. MESSNER and R. W. ZDARKO
Stanford Linear Accelerator Center, Stanford University, Stanford, CA 94309, USA

J. R. JOHNSON

University of Wisconsin, Madison, WI 53706, USA

Presented *by* J. R. Johnson

Abstract

A brief description is given of the SLD calorimeter system, with emphasis on the iron calorimeter/muon identifier. Design choices and expected performance are summarized.

Presented at the 4th Pisa Meeting on Advanced Detectors:

Frontier Detectors for Frontier Physics,

La Biodola, Isola d'Elva, Italy, May 21-26, 1989

*Work supported in part by Department of Energy (USA) contracts DE-AC02-76ER03069 (MIT), DE-AC03-76SF00515 (SLAC), and DE-AC02-76ER00881 (UW), and by the Istituto Nazionale di Fisica Nucleare (Italy).

1. Introduction

The SLC Large Detector (SLD) is a new state-of-the-art general-purpose device for physics studies of e^+e^- annihilation at energies near the Z^0 . Because the SLC has only one interaction region, it is important to combine, in a single detector, the best possible performance in all required aspects: tracking, particle identification, and calorimetry. The first two are satisfied by a precision CCD vertex detector, a high-resolution drift-chamber system, and Cerenkov ring-imaging devices (CRIDs), all in the uniform axial magnetic field of a large solenoid coil. These must then be included within a calorimeter system capable of very good energy and spatial resolution, down to very low particle energies, for both electromagnetic and hadronic particles. There must also be a system for identifying and tracking muons which penetrate the calorimeter. The following sections provide a brief description of the overall design chosen to meet these requirements within a limited budget and schedule, and the construction and performance of the iron calorimeter/muon identifier section. Other details may be found elsewhere [1,2].

2. Calorimeter design choices

2.1. Electromagnetic section

The requirement of good performance for low-energy particles demands that the unsampled material preceding the calorimeter be minimized. In practice, this means that the electromagnetic calorimeter section must be located inside any magnet coil, and this solution was adopted for the SLD. A further choice was to use liquid-argon sampling for this section, since this technique is unaffected by the magnetic field. Liquid argon also does not suffer radiation damage, and since the charge collection mechanism has unit gain, channel-to-channel gain variations can be calibrated very accurately in the electronics. For good containment of high-energy electromagnetic showers (up to 50 GeV), the total

depth of this section was chosen to be 22 radiation lengths of liquid argon plus high-2 absorber plates.

2.2. Hadronic section

The requirement of very good hadron calorimetry then posed a possible problem. The presence of a large coil (about 0.5 nuclear-interaction lengths thick) following 22 radiation lengths would place this unsampled material in the vicinity of the maximum energy deposition in hadron showers, resulting in large fluctuations in the sampled energy. At the same time, the total calorimeter thickness must be at least six interaction lengths for good hadron shower containment and muon filtering. Placing such a large device entirely inside the magnet coil was judged too expensive.

The chosen solution may be termed a “hybrid” hadron calorimeter. First, the liquid-argon calorimeter (LAC) inside the coil is extended to a thickness of about three interaction lengths, using coarser sampling after the electromagnetic section. The LAC will then contain, on average, more than 85% of the-shower energy for most hadrons encountered in SLC events, so that most of the hadronic energy is sampled in a high-quality liquid-argon device. The coil is placed out in the shower tails where the unsampled energy will be small. The coil is then surrounded by an iron-plate calorimeter sampled with plastic streamer tubes (called the WIC, for Warm Iron Calorimeter), which also serves as the magnetic flux return. With 5-cm-thick iron plates and total depth of more than four interaction lengths, this device measures the energy emerging from the LAC plus coil with adequate resolution (about $80\%/\sqrt{E}$, where E = particle energy in GeV), and also serves to identify and track muons. A cross section of the final detector design is shown in fig. 1.

A final choice was the high-2 absorber material for the LAC. Although, in principle, depleted uranium offers the best performance, beam tests and Monte Carlo studies [1,3]

showed that the advantage over lead is small when combined with liquid-argon sampling, and lead was chosen to save large amounts of money, time, and trouble. Sampling thicknesses were set at 2 mm lead in the electromagnetic section and 6 mm in the hadronic part of the LAC. Based on the studies mentioned above, the electromagnetic energy resolution will be better than $10\%/\sqrt{E}$, while the combined hadronic energy resolution in the actual finished detector (including the effect of the coil) is expected to be better than $60\%/\sqrt{E}$.

Details of the LAC construction may be found elsewhere [1], while the remainder of this paper will be devoted to the WIC. More information about the WIC is given in ref. [2].

3. WIC construction

Figure 2 shows schematically the arrangement of streamer-tube sampling chambers in the octagonal barrel section of the iron calorimeter. There are 14 iron plates 5 cm thick, separated by 3.2-cm gaps, into which the chamber planes are inserted. A normal chamber consists of a single layer of plastic streamer tube modules sandwiched between external readout electrode sheets, on which signals are induced by streamer discharges in the modules. Normally, one sheet is an array of quadrilateral pads which are connected with matching pads in other layers to form projective towers matching the LAC (indicated by dashed lines in fig. 1), while the other consists of long narrow strips aligned with the module wires. In addition, double layers following the seventh and fourteenth plates have strips oriented perpendicular to the wires, to provide two-dimensional readout for improved tracking. A single layer precedes the first iron plate in the barrel, to sample the shower particles emerging from the coil. The arrangement in the planar endcaps (see fig. 1) is similar, except that this first layer is omitted. Also, in the endcap chambers

the modules are not laminated directly to the electrode sheets, but are inserted into rectangular sleeves slightly larger than the modules, to provide for convenient removal and exchange.

A cutaway view of one end of a plastic streamer tube module is shown in fig. 3. Molded bridges and bridge covers are located every 35 cm, to center the 100- μ m-diam beryllium-copper wires in the 9 x 9 mm channels of a graphite-coated extruded PVC profile. The eight wires are soldered to a printed-circuit board, where each is connected through a 220 Ω resistor to a high-voltage bus. High-voltage, ground, and gas connections are made through fittings molded into an end-plug, which is sealed into an extruded PVC sleeve to form a gas-tight envelope. The other end is similar, except that there are no high-voltage or ground connections and the PC board has no resistors or bus. About 8700 of these module are required, up to 8.6 m in length, and all those installed are required to pass stringent tests with gas and high voltage. The tests last approximately ten days, and about 25% of the modules are rejected.

The electrode sheets are made from copper-clad fiberglass, with the desired pattern cut into the copper foil on one surface by a computer-controlled routing machine. Figure 4 shows the pattern cut for the longitudinal strip electrodes of barrel chambers, including an edge connector for convenient cabling to electronics. Figure 5 shows typical pad patterns for barrel and endcap chambers. Pad signals are brought out to the chamber ends on flat multiconductor cable (barrel) or traces on a strip of copper-clad fiberglass (endcaps).

The electronic readout of the signals induced on the electrodes is an analog system for the pads (for calorimetry) and digital for the strips (for tracking). The pad connections are ganged at the chamber ends to form projective towers, dividing the azimuth in 96, and subtending about the same interval in polar angle. The towers are divided into two segments in depth, seven layers each except for the outer barrel segment (eight layers).

The signal induced on a tower segment is integrated with a $5 \mu\text{s}$ time constant by a hybrid preamplifier, with the result read by a sample-and-hold circuit and digitized by an ADC. Approximately 8600 channels are required. The strips are read out individually (about 80,000 channels) using a preamplifier/discriminator/shift-register -system described in detail elsewhere [4]. The solid-angle coverage for both systems is 99.2% of 4π .

4. WIC status and performance

As of the time of this conference, all the WIC chambers have been built, and almost all of them have been tested with cosmic rays and then installed in the iron structure. The total area covered is about 4500 sq m, and the total gas volume is about 33 cu m. Commissioning in place with gas, high-voltage, and strip-readout electronics has been proceeding since September 1988, using a new nonflammable gas mixture [5] consisting of 88% CO_2 , 9.5% isobutane, and 2.5% argon. Fewer than 1% of the modules commissioned so far have been judged inoperable, except in certain areas of mechanical stress due to installation. Failed modules are disconnected or replaced. Note that in some cases nearly two years had elapsed between cosmic-ray tests and commissioning. Electronic noise and pickup have been found to be manageable, and cosmic-ray tracks are routinely recorded in the barrel section. Figure 6 shows one example, with only six planes recorded due to the temporary nature of the data acquisition system.

The expected performance of the WIC as a hadron calorimeter has been measured in beam tests [6]. In agreement with similar measurements by other groups, the energy resolution is about $\sigma_E/E = 80\%/\sqrt{E}$. The tracking performance of actual chambers has been tested extensively with cosmic rays. Figure 7 shows, for example, the hit efficiency and position resolution for a single plane with 1-cm-wide strips along the wires, as a function of the angle of the cosmic ray from the normal to the chamber in a plane

perpendicular to the wire. For normal incidence, the inefficiency is about 10%, due to the dead space of channel walls and sleeves. As the angle increases, it is more likely that the track will pass through more than one cell, so the efficiency improves; but eventually the resolution deteriorates.

Since the iron plates of the WIC barrel are magnetized parallel to the chamber wires, the tracking capability of the longitudinal strip readout may be used to measure the momentum of penetrating muons. Figure 8 shows the result of a Monte Carlo study of the momentum resolution achievable in the barrel section. It can be seen that charge determination is possible for momenta below about 13 GeV/c, and muon identification will be aided by comparison with momenta measured in the SLD central drift chamber.

5. Summary

Through the use of a “hybrid” hadron calorimeter design, the SLD calorimeter system will be able to provide excellent performance in all aspects needed for a competitive physics program at SLC energies, including hermetic coverage over 99% of 4 π solid-angle, projective tower segmentation, and unusually good electromagnetic and hadronic energy resolution for such a large general-purpose magnetic detector:

$$\frac{\sigma_E}{E} \text{ (electromagnetic)} \leq \frac{10\%}{\sqrt{E}} ,$$

$$\frac{\sigma_E}{E} \text{ (hadronic)} \leq \frac{60\%}{\sqrt{E}} .$$

In addition to providing part of the hadronic energy measurement, the iron calorimeter adds muon identification, tracking, and momentum measurement.

Acknowledgments

The successful design and construction of the WIC could not have been accomplished without the help of a large number of skilled people. Particular thanks are due to F. Babucci, G. Bonora, U. Cazzola, D. Ross and D. Sawyer for their dedicated efforts and contributions. The authors would also like to acknowledge the able technical assistance of the following: V. Giordano and A. Zucchini (Bologna); S. Bigoni, V. D'Orto and C. Fordiani (Ferrara); D. Pistoni (Frascati); the Campana crew (MIT); G. Marinolli, B. Migliorato and A. Paonessa (Padova); E. Babucci and G. Chiocci (Perugia); F. Bosi, L. Corucci, G. Fausto and L. Zaccarelli (Pisa); and N. Erickson, J. Escalera, M. Mittmann and P. Ritson, as well as the crews at IR-6 and the Light Assembly Building (SLAC). In addition, we would like to express our appreciation for the extensive use of the routing machinery at the Fermi National Accelerator Laboratory.

This work was supported in part by Department of Energy (USA) contracts DE-AC02-76ER03069 (MIT), DE-AC03-76SF00515 (SLAC), and DE-AC02-76ER00881 (UW), and by the Istituto Nazionale di Fisica Nucleare (Italy).

References

- [1] SLD Design Report, SLAC Report SLAC-273 (1984).
- [2] A. C. Benvenuti et al., Nucl. Instr. and Meth. A276 (1989) 94.
- [3] R. Dubois et al., IEEE Trans. Nucl. Sci. NS-33 (1986) 194.
- [4] P. G. Verdini, for the SLD-WIC collaboration, paper presented at this conference.
- [5] S. Cartwright et al., Nucl. Instr. and Meth. A277 (1989) 269;
A. C. Benvenuti et al., SLAC preprint SLAC-PUB-4687 (1989), to be published in Nucl. Instr. and Meth.
- [6] G. Callegari et al., IEEE Trans. Nucl. Sci. NS-33 (1986) 201.

Figure Captions

Fig. 1. One quadrant of a cross-section of the SLD detector. The dashed lines in the LAC indicate boundaries of the projective towers, which are matched in the WIC. The barrel WIC is in the form of an octagonal cylinder.

Fig. 2. Arrangement of chamber layers in a typical barrel octant of the WIC. The endcap arrangement is similar.

Fig. 3. S-Cutaway view of one end of a plastic streamer-tube module.

Fig. 4. Longitudinal strip electrode pattern for barrel chambers.

Fig. 5. Pad patterns for (a) one-half of a typical layer in a barrel octant (the other is a mirror image), and (b) one quadrant of a typical endcap layer.

Fig. 6. A cosmic-ray event in six layers of a barrel octant. Boundaries of individual chamber units are shown, and small vertical dashes indicate the positions of longitudinal strips with signal above threshold.

Fig. 7. (a) The efficiency of a single chamber layer for recording the passage of a cosmic-ray muon, as a function of the muon azimuthal angle about the wire direction, measured from the normal to the chamber plane. (b) As a function of this same angle, the graph shows the measured resolution in a single layer for determining the muon position (transverse to the wire direction) from the pattern of 1-cm-wide longitudinal strips with signal above threshold. The resolution is given as a ratio to the limiting value $1 \text{ cm}/\sqrt{12}$.

Fig. 8. Momentum resolution for muons tracked through the magnetized iron of the WIC barrel, as a function of the muon momentum. The values were calculated from a Monte Carlo detector simulation.

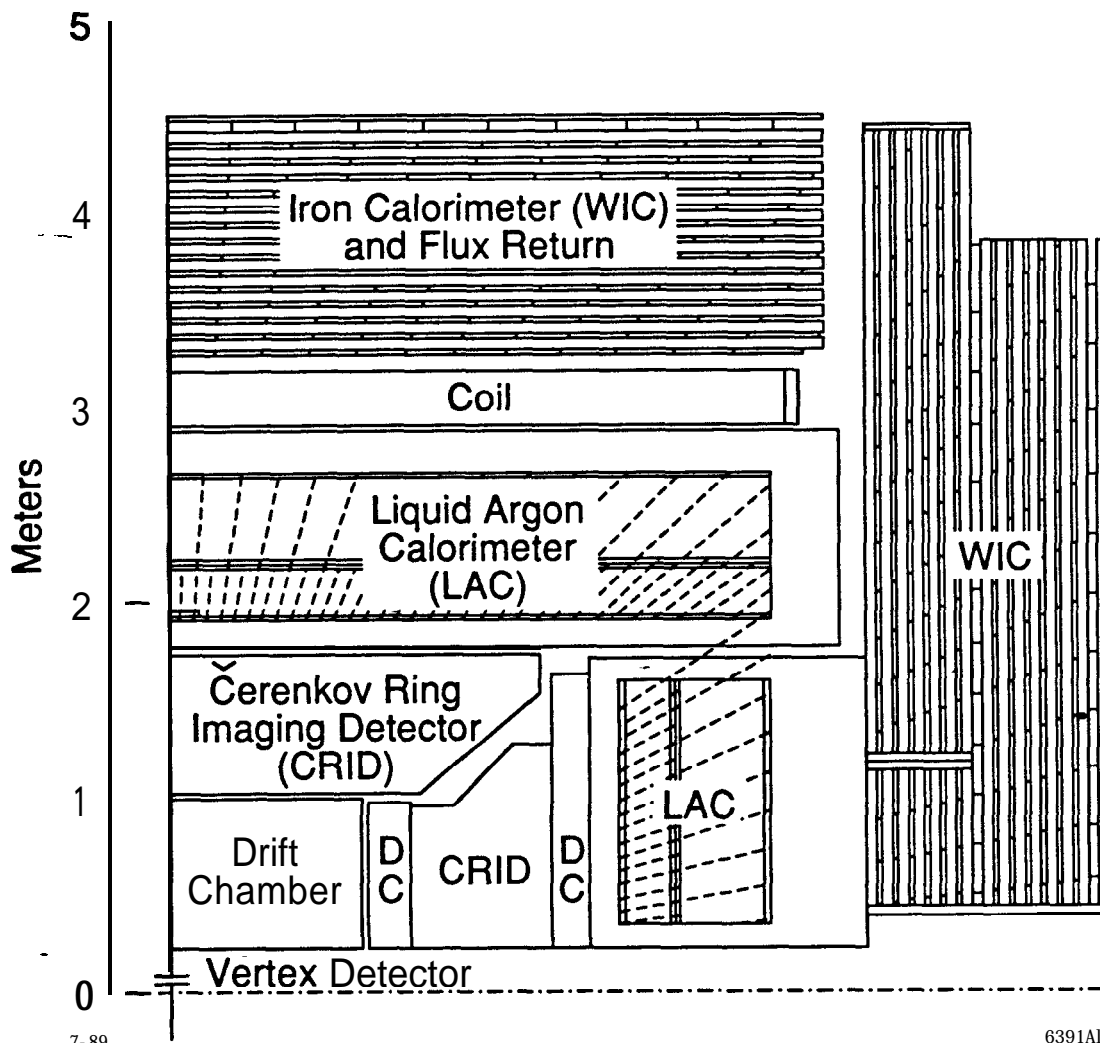
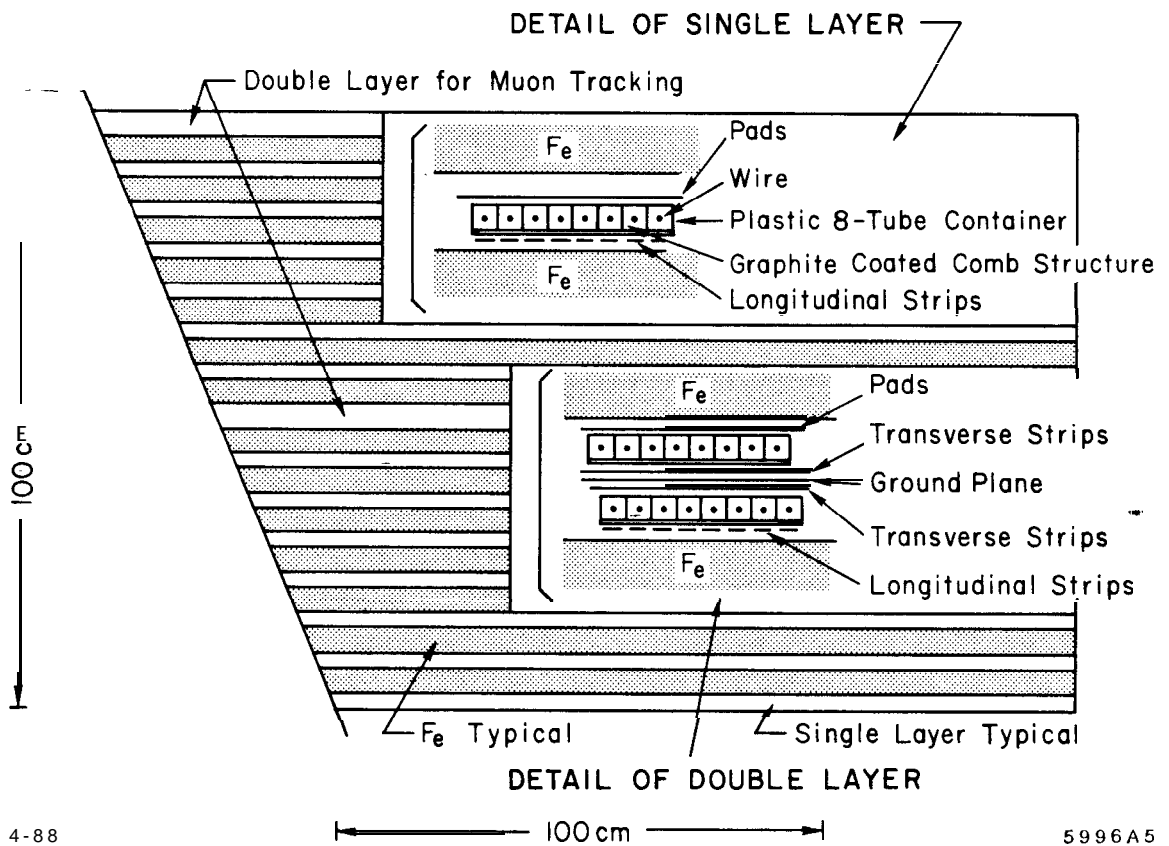


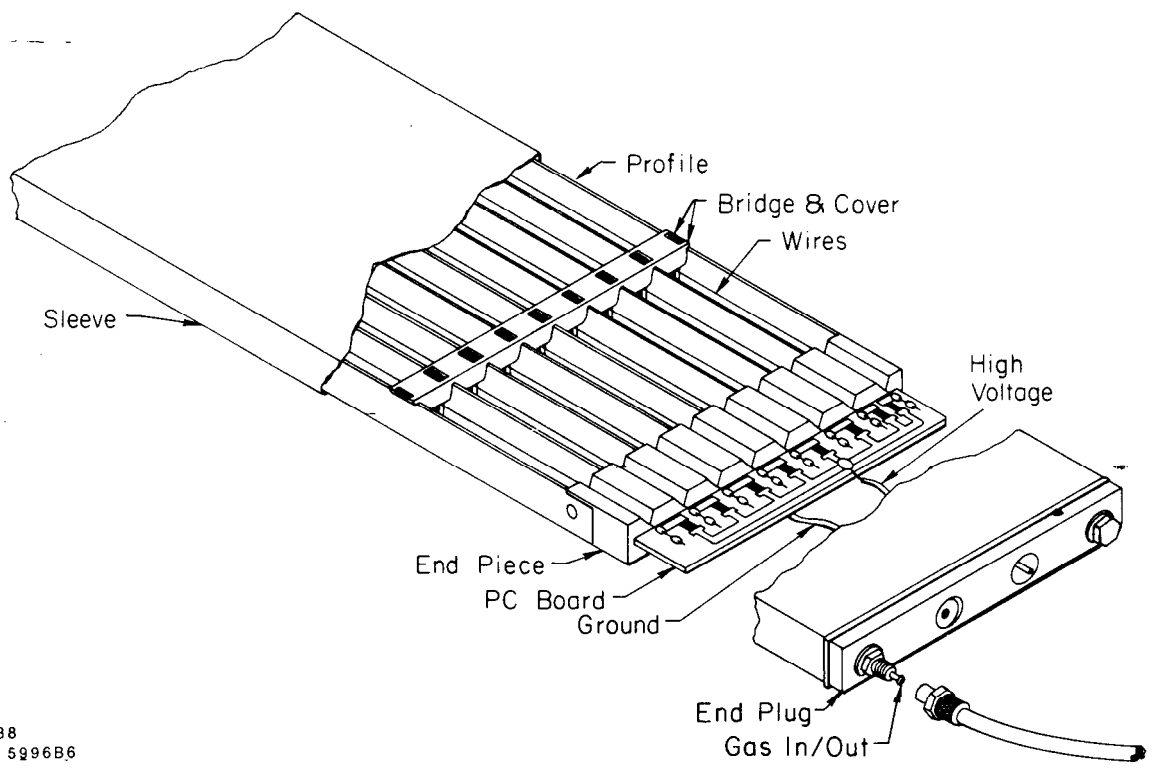
Fig. 1



4-88

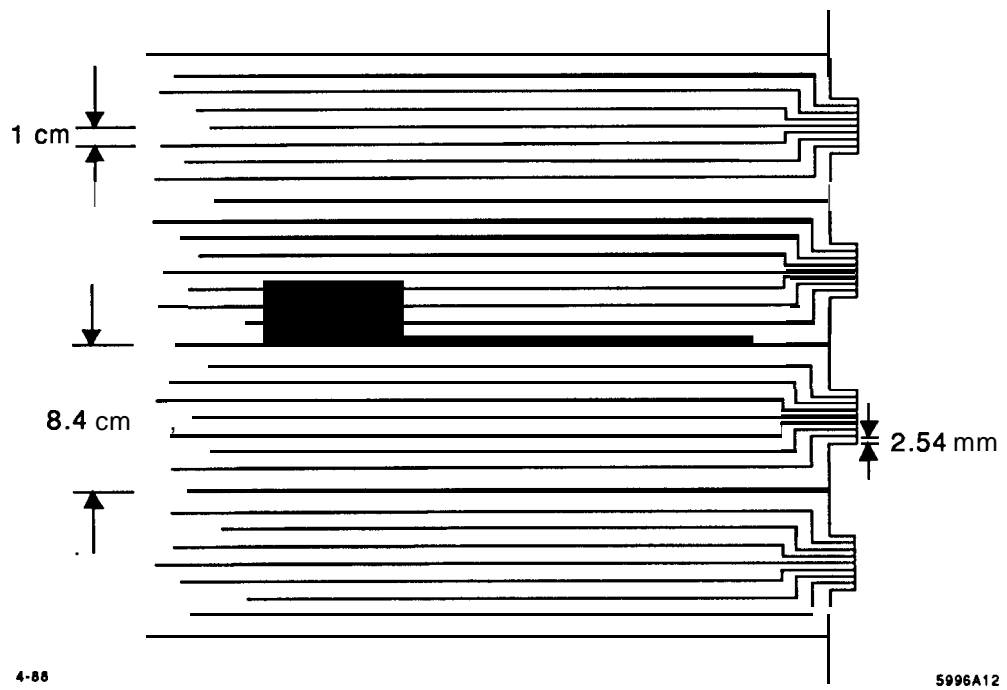
5996A5

Fig. 2



4-88
5996B6

Fig. 3



4-88

5996A12

Fig. 4

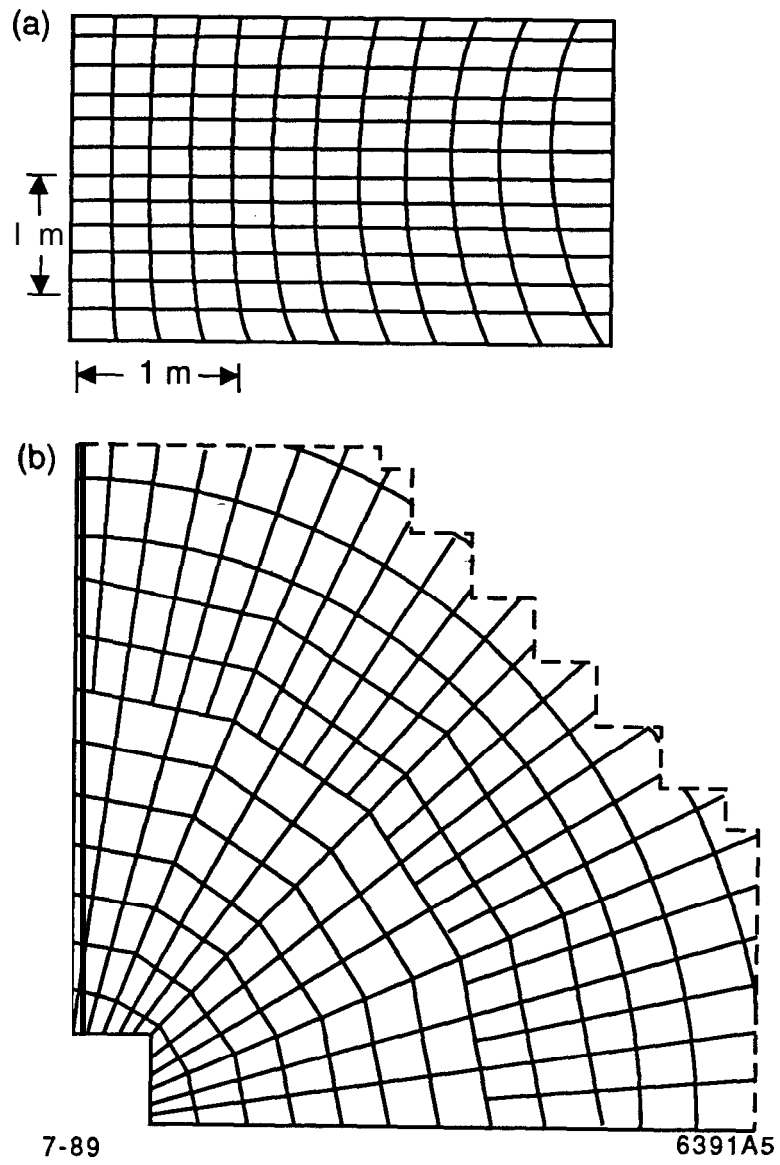
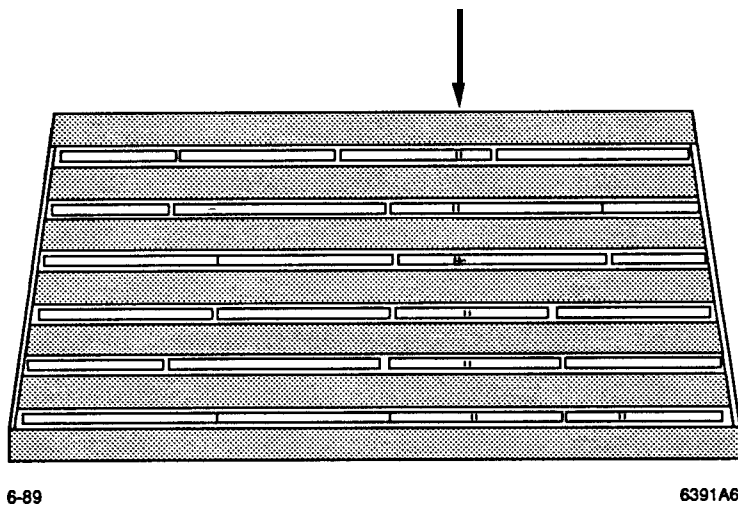


Fig. 5



6-89

6391A6

Fig. 6

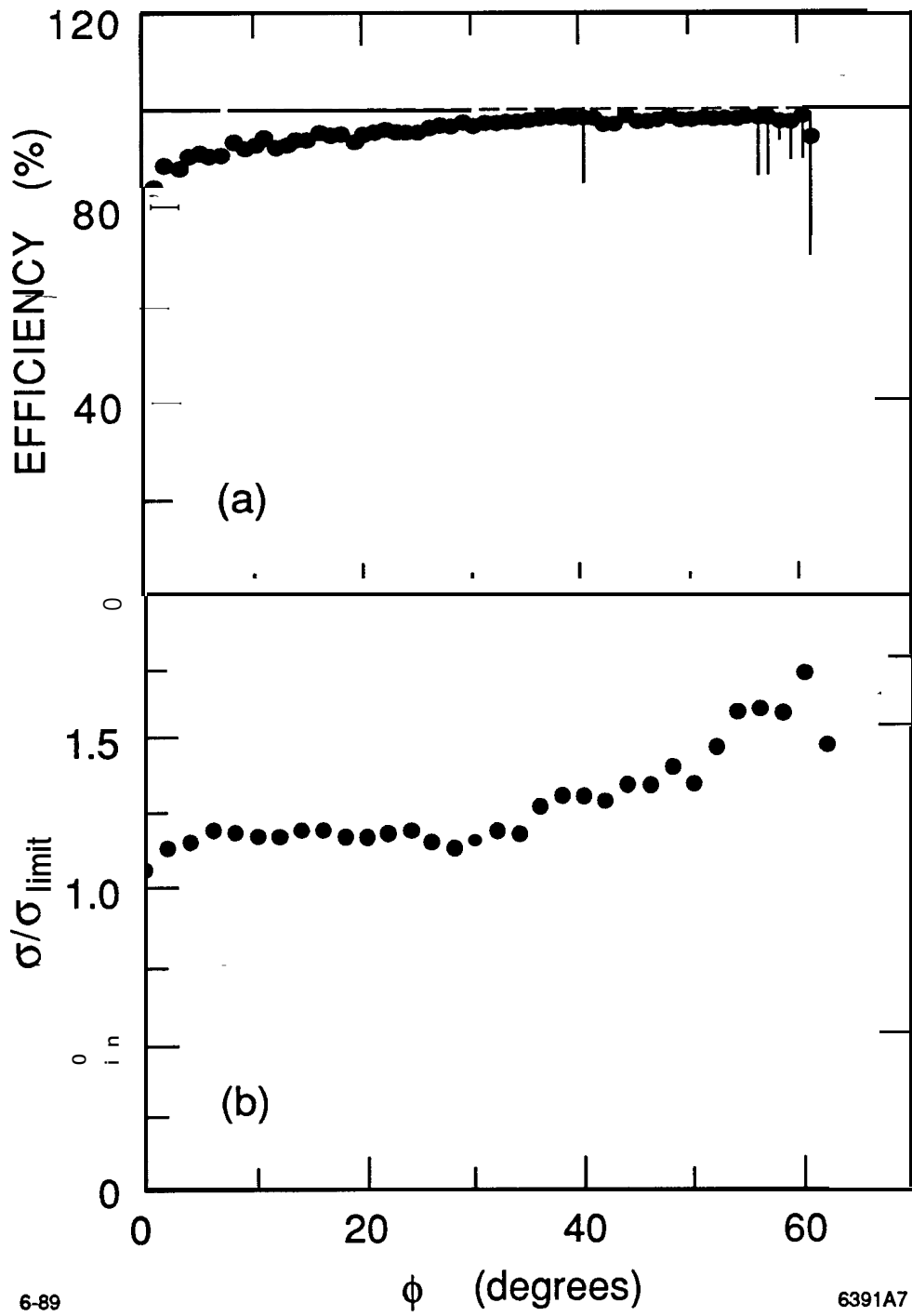
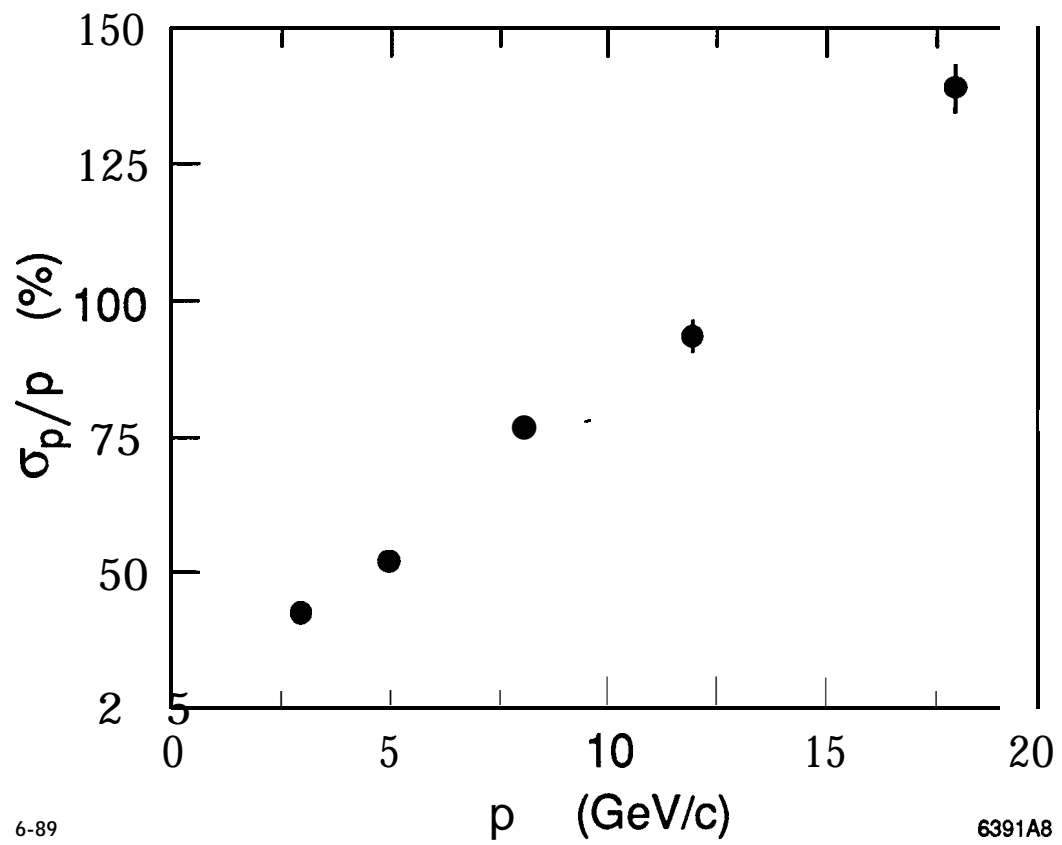


Fig. 7



6-89

6391A8

Fig. 8